UDK 620.193:669.14:669.245
Original scientific article/Izvirni znanstveni članek

ISSN 1580-2949
MTAEC9, 40(6)247(2006)

THE STABILITY OF CAST ALLOYS AND CVD COATINGS IN A SIMULATED BIOMASS-COMBUSTION ATMOSPHERE

STABILNOST ZLITIN IN CVD-PREVLEK V SIMULIRANI ATMOSFERI ZGOREVANJA BIOMAS

Danijela A. Skobir[1], **Michael Spiegel**[2]
[1]Institute of Metals and Technology, Lepi pot 11, SI-1000 Ljubljana, Slovenia
[2]Max-Planck-Institut für Eisenforschung GmbH, Max-Planck-Straße 1, D-40237 Düsseldorf, Germany
danijela.skobir@imt.si

Prejem rokopisa – received: 2006-09-29; sprejem za objavo – accepted for publication: 2006-10-13

The corrosion resistance in a biomass-combustion environment was studied for the following materials: cast alloys (Alloy 800, Inconel 617, 1.4910, HCM 12 and P91), Fe-9 % Cr model alloys with and without additions of Al, Si and Mo, and cast alloys coated using the pack-cementation process with Al and Al-Si. The simulated atmosphere for the biomass-combustion environment contained 200 µg/g HCl, volume fractions 13 % CO_2, 22 % H_2O and 5 % O_2. The samples were covered with a salt mixture of mass fractions of 52.4 % KCl and 47.6 % K_2SO_4 in order to simulate the corrosion beneath the deposits. The specimens were exposed for 1000 h at the test temperature of 550 °C.

Keywords: hot corrosion, biomass combustion, CVD-coatings, deposits

S korozijskimi preizkusi v simulirani atmosferi za zgorevanje biomas smo raziskovali korozijsko obstojnost naslednjih materialov: lite zlitine (zlitina 800, Inconel 617, 1.4910, HCM 12 in P91), modelne zlitine Fe-9 % Cr z dodatki Al, Si in Mo in brez njih ter lite zlitine, na katere je bila s CVD-postopkom nanesena plast Al oziroma Al-Si. Simulirana atmosfera za zgorevanje biomas je vsebovala 200 µg/g HCl in prostorninske deleže: 13 % CO_2, 22 % H_2O in 5 % O_2. Vzorci so bili prekriti s solno mešanico z masnima deležema 52,4 % KCl in 47,6 % K_2SO_4 za simulacijo korozije pod depoziti. Preizkusi so potekali pri temperaturi 550 °C, čas trajanja preizkusov pa je bil 1000 h.

Ključne besede: visokotemperaturna korozija, zgorevanje biomas, CVD-prevleke, depoziti

1 INTRODUCTION

One of the most important problems of modern society is the removal of waste and biomass, stemming mainly from the production of highly developed industrial products. An effective and useful way of removing biomass is combustion, connected with the production of steam used for the production of electrical energy. Nowadays, approximately 23 % of the total amount of waste in Europe is burned; the rest is deposited in landfills[1,2]. In Western Europe, nearly 600 combustion plants are in operation, and the number is still increasing. Until 2010 an increase in the total amount of energy from renewable sources, from 6 % to 12 %, is expected, as well as a substantial increase in the efficiency of thermal power plants.

Corrosion is a major issue concerning the limited lifetime of tube materials and the plant efficiency in biomass- and waste-incineration plants. In biomass-fired plants, high contents of potassium and chlorine are present in the combustion environment, causing early failure of the thermal components, such as superheater tubes[3,4]. Solid and/or liquid chloride salts, together with their vapours, can destroy the protective surface oxide scales of high-temperature materials, even at temperatures well below the melting points of the salts[2, 5-7]. Rapid corrosion results from the complicated chemical reactions between tube materials and the gaseous species (HCl, SO_2, etc.) and, especially, the low melting point of the eutectic salts of heavy metals (Sn, Pb, Zn) and alkali-metal (K, Na) chlorides, as well as sulfates[2, 8-10]. The most corrosive species in the flue gas is HCl. There is generally more HCl than SO_2; however, the HCl/SO_2 ratio strongly depends on the waste being burned. A generally accepted model for chlorine-induced corrosion in waste- and biomass-fired boilers is the 'active oxidation' mechanism, first observed and described by Lee and McNallan[11]. The chlorine is produced by the catalytic oxidation of HCl according to Deacon reaction (Eq. 1) as well as by the reaction of the salt with the oxide scale of the pre-oxidized metal, according to Eq. 2 and 3:

$$2HCl + 1/2O_2 = H_2O + Cl_2 \quad (1)$$

$$2NaCl + Fe_2O_3 + 1/2O_2 = Na_2Fe_2O_4 + Cl_2 \quad (2)$$

$$2NaCl + Cr_2O_3 + 1/2O_2 = Na_2Cr_2O_4 + Cl_2 \quad (3)$$

The chlorine diffuses through the cracks and pores of the oxide scale to the metal/scale interface, reacting to form $FeCl_2(s)$:

$$Fe + Cl_2 = FeCl_2(s) \rightarrow FeCl_2(g) \quad (4)$$

As the vapor pressure of the chloride is 10^{-4} bar at 500 °C, it evaporates and the volatile chloride diffuses

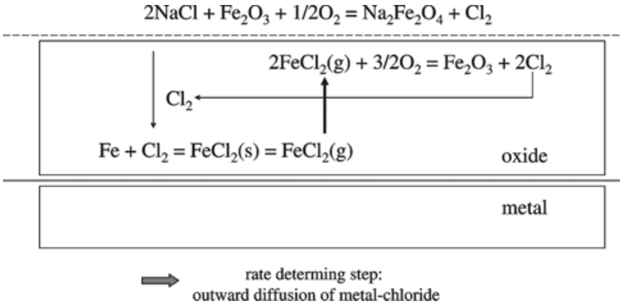

Figure 1: Schematic model of the mechanism of "active oxidation"
Slika 1: Shematski prikaz modela "aktivne oksidacije"

outwards through the oxide scale. At the oxide/gas interface the reaction to Fe_2O_3 takes place, releasing chlorine again:

$$2FeCl_2(g) + 3/2O_2 = Fe_2O_3 + 2Cl_2 \quad (5)$$

The growth of the Fe_2O_3 in the cracks and pores of the oxide destroys the scale and the corrosive gas can react with the unprotected metal. Hence, a scale is produced on the metal substrate, which is not passivating and, for this reason, the mechanism was nominated as active oxidation. The mechanism of this oxidation is schematically presented in **Figure 1**. The chlorine plays a catalytic role in this corrosion process because it is not consumed. In-depth thermogravimetric studies on the mechanism of active oxidation were carried out by Reese and Grabke[12], showing that the evaporation of $FeCl_2(g)$ from the metal/scale interface is the rate-determining step in NaCl-induced corrosion. In order to increase the efficiency of combustion plants it is necessary to develop effective protective coatings for vital components in hostile combustion environments.

2 EXPERIMENTAL

In this study, bare metals, CVD coatings and model alloys were tested in a simulated biomass-combustion atmosphere. The chemical composition of the cast alloys is presented in **Table 1**. All of these alloys are based on iron, except for Inconel 617, which is a nickel-based alloy.

With the goal to decrease the surface degradation that occurs on exposure to high temperatures and corrosive atmospheres the cast alloys were coated using the pack-cementation process. The results of the exposure tests of uncoated as well as coated alloys were compared.

The pack-cementation process is essentially an *in-situ* chemical vapour deposition (CVD) process, which is used to deposit Al or some other elements (Al-Si, Al-Cr and Al-B) onto metal substrates to form aluminide diffusion coatings.

The substrates to be coated were placed in a sealed or semi-sealed container together with a powder mixture that consists of metal elements to be deposited (diffusion element), a halide activator (NH_4Cl) and an inert filler (Al_2O_3). The substrates can be buried in, or placed above, the powder mixture. The sealed container is heated under a protective atmosphere of Ar to a temperature between 650–1200 °C and held there for a specified time. At these coating temperatures the halide activators react with the metal elements in the powder mixture and form a series of metal-halide vapour species such as AlCl, $AlCl_2$, $AlCl_3$ and Al_2Cl_6[13]. The coating is formed via reduction reactions of the metal-halide vapours at the substrate surface and subsequent solid-state diffusion between the metal elements and the substrate. For this reason, the coatings produced by using this process are also termed diffusion coatings.

Additionally, Fe-9 % Cr model alloys with and without additions of Al, Si and Mo were tested under the same conditions. The chemical composition of the model alloys is presented in **Table 2**.

All the materials were machined into specimens with dimensions of about (10 × 10 × 2) mm, then ground with 400 # and 600 # SiC paper, cleaned in a ultrasonic bath

Table 1: Chemical composition of the cast alloys (*w*/%)
Tabela 1: Kemijska sestava litih zlitin (*w*/%)

Alloy	Cr	Ni	Fe	Mn	Mo	Al	Co	Si	V
Alloy 800	19–23	30–34	bal	<1.5	-	0.1–0.6	-	0.5	-
Inconel 617	20–24	bal	max 3	max 1	8–10	-	10–15	max 1	-
1.4910	16–18	12–14	bal	<2	2–2.5	-	-	<0.75	-
HCM 12	11.2	0.66	bal	0.50	0.86	-	-	-	0.25
P 91	8.6	0.26	bal	0.41	0.93	-	-	0.3	0.21

Table 2: Chemical composition of the model alloys (*w*/%)
Tabela 2: Kemijska sestava modelnih zlitin (*w*/%)

Alloy	Fe	Cr	Mo	Al	Si
VI811	bal	9	-	2.5	2.5
VI813	bal	9	10	-	-
VI814	bal	9	10	2.5	2.5
VI815	bal	9	5	2.5	2.5

of acetone and weighed. After drying, each sample was covered with a salt mixture of mass fractions 52.4 % KCl and 47.6 % K_2SO_4 to simulate the corrosion beneath deposits.

The exposure experiments were performed in a flue-gas, using a horizontal furnace equipped with a quartz working tube. The furnace was connected to gas-mixing equipment; however, the N_2–5 % O_2–200 µg/g HCl mixture was supplied as a premixed commercial gas. The gas was dried by passing it through columns filled with P_2O_5 before entering the furnace. Because of the large constant-temperature zone it was possible to test 20 samples at the same time. The exposure experiments were carried out at 550 °C. The extent of the corrosion was determined by measuring the mass loss after 1000 h of reaction after the removal of the corrosion products by chemically etching in a $KMnO_4$-NaOH solution at 80 °C. After exposure, metallographic cross-sections were prepared by dry grinding the samples in order to prevent the dissolution of the chloride products from the scale. Scanning electron microscopy (SEM) and energy-dispersive X-ray analysis (EDX) were used to study the morphology and the chemical composition of the corrosion products.

3 RESULTS AND DISCUSSION

Figure 2 shows the extent of the corrosion on the investigated alloys, expressed in terms of mass change in mg/cm^2. The model alloys, VI814 and VI815, show a relatively small mass loss for the samples in the biomass-combustion environment due to their high content of Al, Si and Mo. The corrosion layer on the SEM micrograph of a cross-section of the VI815 alloy (**Figure 3a**) is very thin, about 52 µm. The corrosion layer consists of an Fe-rich layer and closer to the metal there is a scale interface, with an increasing amount of Cr, Al, Si and Mo being detected. The inner part is a Cr-rich layer with a large amount of Cl (**Figure 3b**).

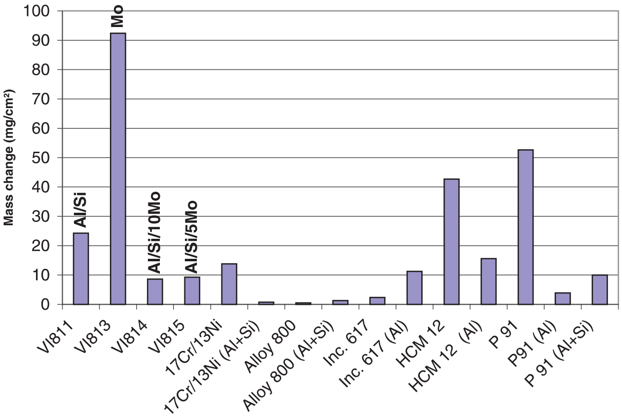

Figure 2: Mass loss of the materials exposed in a flue gas for 1000 h at 550 °C and covered with the KCl-K_2SO_4 salt mixture

Slika 2: Sprememba mase preizkušancev po 1000-urnem korozijskem preizkusu na 550 °C pod depozitom solne mešanice KCl-K_2SO_4

Slightly worse corrosion behavior was shown by the VI811 alloy, whereas the VI813 alloy with a high Mo content was almost completely corroded. The analysis of the deposited layer of the VI813 alloy shows that the corrosion layer consists of two sublayers and is very thick, about 622 µm (**Figure 4a**). In the upper layer is the remainder of the salt on the top, and below an Fe-oxide was formed, where no chromium was found. The underneath layer is the layer of the inner corrosion products. **Figure 4b** shows a detailed view of the internal oxidation zone, which is relatively deep and therefore responsible for the large mass loss. The outer part of the scale of inner corrosion products is an Fe-rich layer, and towards the metal-scale interface an increasing content of Cr, Cl and Mo and no sulphur were detected.

From **Figure 2** it can also be seen that the corrosive attack on the nickel-based Inconel 617 alloy and on the 800 alloy with the high Ni content is much smaller than on the iron-based cast alloys. From **Figure 5a** it is clear that the corrosion layer on the exposed Inconel 617 is extremely thin, only about 3.6 µm, which shows that this alloy is just slightly corroded. The corrosion layer consists of two layers (**Figure 5b**): the first layer is the Ni-rich layer, and the second is the Cr-rich layer below. No chlorides were detected in this layer.

The corrosion layer for the cast P91 alloy (**Figure 6a**), which has the lowest corrosion resistance among the

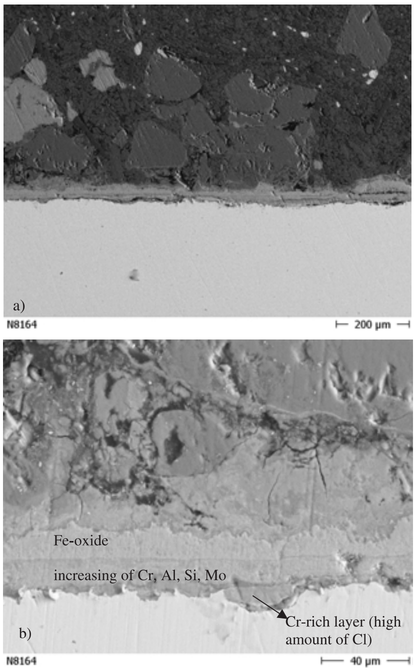

Figure 3: SEM micrograph from a metallographic cross-section of the VI815 model alloy after corrosion beneath the KCl-K_2SO_4 salt mixture in N_2-5 % O_2-200 µg/g HCl at 550 °C for 1000 h. (a) overview image; (b) detailed image of the internal part of the corrosion layer

Slika 3: SEM-posnetek metalografskega prereza za modelno zlitino VI815 po koroziji pod solno mešanico KCl-K_2SO_4 v N_2-5 % O_2-200 µg/g HCl pri 550 °C in po 1000 h. (a) pregledna slika; (b) detajlna slika notranjega dela korozijske plasti

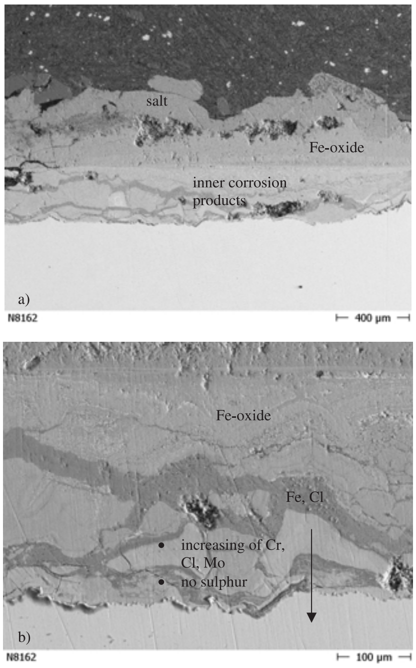

Figure 4: SEM micrograph from a metallographic cross-section of the VI813 model alloy after corrosion beneath the KCl-K_2SO_4 salt mixture in N_2-5 % O_2-200 µg/g HCl at 550 °C for 1000 h. (a) overview image; (b) detailed image of the internal part of the corrosion layer

Slika 4: SEM-posnetek metalografskega prereza za modelno zlitino VI813 po koroziji pod solno mešanico KCl-K_2SO_4 v N_2-5 % O_2-200 µg/g HCl pri 550 °C in po 1000 h. (a) pregledna slika; (b) detajlna slika notranjega dela korozijske plasti

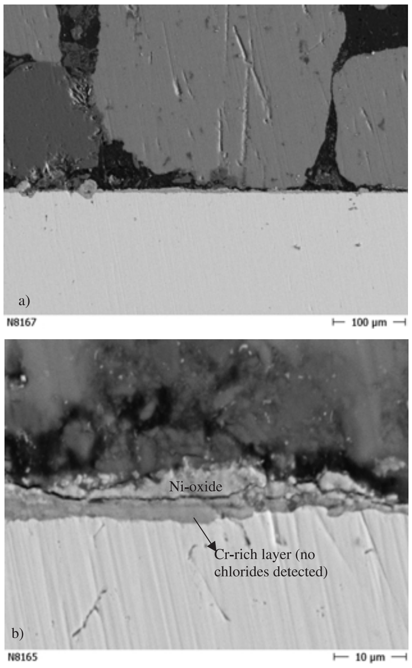

Figure 5: SEM micrograph from a metallographic cross-section of the Inconel 617 alloy after corrosion beneath the KCl-K_2SO_4 salt mixture in N_2-5 % O_2-200 µg/g HCl at 550 °C for 1000 h. (a) overview image; (b) detailed image of the internal part of the corrosion layer

Slika 5: SEM-posnetek metalografskega prereza za zlitino Inconel 617 po koroziji pod solno mešanico KCl-K_2SO_4 v N_2-5 % O_2-200 µg/g HCl pri 550 °C in po 1000 h. (a) pregledna slika; (b) detajlna slika notranjega dela korozijske plasti

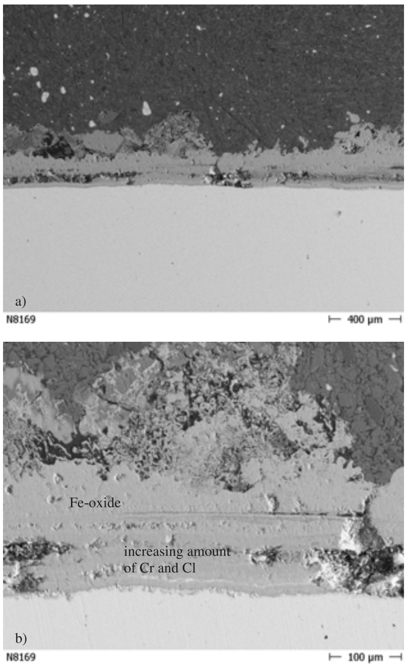

Figure 6: SEM micrograph from a metallographic cross-section of the P91 alloy after corrosion beneath the KCl-K_2SO_4 salt mixture in N_2-5 % O_2-200 µg/g HCl at 550 °C for 1000 h. (a) overview image; (b) detailed image of the internal part of the corrosion layer

Slika 6: SEM-posnetek metalografskega prereza za zlitino P91 po koroziji pod solno mešanico KCl-K_2SO_4 v N_2-5 % O_2-200 µg/g HCl pri 550 °C in po 1000 h. (a) pregledna slika; (b) detajlna slika notranjega dela korozijske plasti

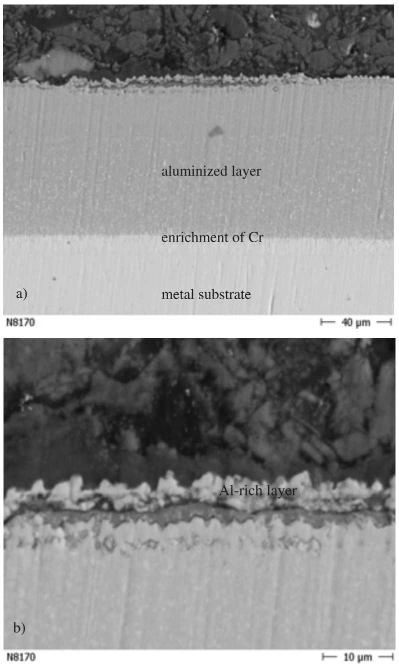

Figure 7: SEM micrograph from a metallographic cross-section of Al-coated Inconel 617 alloy after corrosion beneath the KCl-K_2SO_4 salt mixture in N_2-5 % O_2-200 µg/g HCl at 550 °C for 1000 h. (a) overview image; (b) detailed image of the internal part of the corrosion layer

Slika 7: SEM-posnetek metalografskega prereza za zlitino Inconel 617, prevlečeno z Al po koroziji pod solno mešanico KCl-K_2SO_4 v N_2-5 % O_2-200 µg/g HCl pri 550 °C in po 1000 h. (a) pregledna slika; (b) detajlna slika notranjega dela korozijske plasti

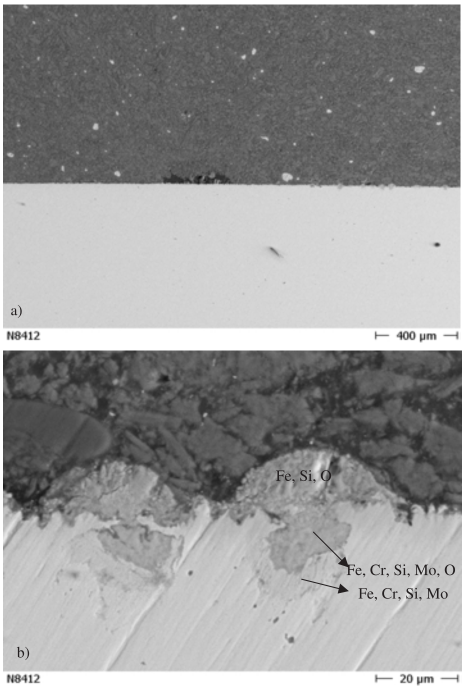

Figure 8: SEM micrograph from a metallographic cross-section of the P91 alloy, coated with Al-Si after corrosion beneath the KCl-K$_2$SO$_4$ salt mixture in N$_2$-5 % O$_2$-200 µg/g HCl at 550 °C for 1000 h. (a) overview image; (b) detailed image of the internal part of the corrosion layer

Slika 8: SEM-posnetek metalografskega prereza za zlitino P91, prevlečeno z Al-Si po koroziji pod solno mešanico KCl-K$_2$SO$_4$ v N$_2$-5 % O$_2$-200 µg/g HCl pri 550 °C in po 1000 h. (a) pregledna slika; (b) detajlna slika notranjega dela korozijske plasti

cast alloys, is much thicker (244 µm) than that on the Inconel 617. On the SEM micrograph, again an Fe-rich layer was detected on the top, and an increasing amount of Cr and Cl was detected towards the metal-scale interface (**Figure 6b**).

The exposure tests of Al-coated Inconel 617 and Al-Si-coated 800 alloy did not show any improvement in corrosion resistance compared to the uncoated material (**Figure 2**). In the case of the Inconel 617, coated with Al, there is almost no corrosion layer formed (**Figure 7a**). The aluminised layer (**Figure 7b**) has the chemical composition 36.2 % Al, 35.4 % Ni, 13.7 % Cr, 7.3 % Co, 6.6 % Mo and 0.77 % Fe. Just below this layer an enrichment of Cr was detected. The chemical composition of this layer is 33.9 % Cr, 4.6 % Al, 27.6 % Ni, 11.6 % Co and 19.1 % Mo. Below this layer is the metal substrate.

For all the other coated cast alloys an improvement in the corrosion resistance was observed (**Figure 2**). **Figures 8a** and **b** show the corrosion layer of the P91 alloy, coated with Al-Si.

In spite the fact that the Al-Si coatings were not as thick as the Al coatings (the Al coatings were about 80 µm and Al-Si about 30–40 µm) no significant differences in the corrosion resistance were observed.

4 CONCLUSIONS

Exposure tests were carried out to compare the corrosion resistance of several iron- and nickel-based alloys, as well as the same alloys coated with Al, Al-Si and Fe-9 % Cr model alloys beneath a salt mixture of KCl and K$_2$SO$_4$ in N$_2$–5 % O$_2$ atmosphere with the addition of 200 µg/g HCl. In this atmosphere, which is typical for a biomass-combustion environment, active oxidation by the HCl and alkali-chlorides plays a major role in the corrosion of this material. The results showed that among the model alloys (Fe-9Cr) the most corrosion-resistant are the VI814 and VI815 alloys, due to their large amount of Al, Si and Mo. In the group of cast alloys, the Inconel 617 nickel-based alloy has the best corrosion resistance, followed by the 800 alloy, which also contains quite large amounts of Ni. The Inconel 617 alloy coated with Al, and the 800 alloy coated with Al-Si do not show any improvement in corrosion resistance compared to the uncoated alloys. It can therefore be summarized that the alloying elements Ni, Mo, Al and Si have a beneficial effect on the corrosion resistance of the model and cast alloys. The coatings on the alloys that do not include these alloying elements do not improve the corrosion resistance. The formation of deposits significantly contributes to the corrosion by solid and liquid salts (i.e., chlorides and sulphates).

ACKNOWLEDGEMENTS

This work was carried out within the SUNASPO-Research Training Network at the Department of Interface Chemistry and Surface Engineering of the Max-Planck-Institut für Eisenforschung GmbH, Düsseldorf, Germany. The author would like to thank PD Dr. Michael Spiegel for the opportunity of working in the field of High Temperature Corrosion, and especially for his support. The financial support of the European Commission is gratefully acknowledged.

5 REFERENCES

[1] Statistisches Bundesamt Wiesbaden (**1992**), Statistik der öffentlichen Abfallbeseitigung von 1990

[2] Spiegel M.: Materials and Corrosion 50 (**1999**), 373–393

[3] Sander B.: Biomass and Bioenergy 122 (**1997**), 177

[4] Nielsen H. P., Frandsen F. J., Dam-Johansen K. and Baxter L. L.: Prog Energy Combust Sci. 26 (**2000**), 283

[5] Grabke H. J.: Incinerating municipal and industrial waste in Bryers (ed.), Hemisphere Publ. Corp., (**1991**), 161–176

[6] Li Y. S., Niu Y. and Wu W. T.: Mater. Sci. Eng A345 (**2003**), 64

[7] Shinata Y.: Oxid. Met. 27 (**1987**), 315

[8] Montgomery M. and Karlsson A.: Materials and Corrosion 50 (**1999**), 579

[9] Miller P. D. and Krouse H. H.: Corrosion 28 (**1972**), 274

[10] Grabke H. J., Reese E. and Spiegel M.: Corros. Sci. 37 (**1995**), 1023

[11] Lee Y. Y., McNallan M. J.: Metallurg. Trans. 18A (**1987**), 1099

[12] Reese E., Grabke H. J.: Materials and Corrosion 43 (**1992**), 547

[13] Xiang Z. D., Burnell-Gray J. S. and Datta P. K.: Journal of Material Science 36 (**2001**), 5673